2024 International Conference on Quantum Communications, Networking, and Computing (QCNC) | 979-8-3503-6677-8/24/$31.00 ©2024 IEEE | DOI: 10.1109/QCNC62729.2024.00031

Entanglement Percolation in Noisy Quantum Networks

Soo Min Oh*, Hyundong Shin†, Stefano Marano‡, Andrea Conti§, and Moe Win††

*Wireless Information and Network Sciences Laboratory, Massachusetts Institute of Technology, Cambridge, MA, USA
†Department of Electronics and Information Convergence Engineering, Kyung Hee University, Yongin, South Korea
‡Department of Information & Electrical Engineering and Applied Mathematics, University of Salerno, Fisciano, Italy
§Department of Engineering and CNIT, University of Ferrara, Ferrara, Italy
††Laboratory for Information and Decision Systems, Massachusetts Institute of Technology, Cambridge, MA, USA

***Abstract*—Quantum networks (QNs) are expected to play a key role in next-generation networks. A QN is comprised of quantum nodes and links (or bonds) representing entangled qubit pairs (EQPs) shared between two nodes. The probability of establishing a pure maximally entangled pair, known as Einstein–Podolsky–Rosen (EPR) pair, between two neighboring nodes represents the linking probability (or bond occupation probability). If such probability exceeds the so-called percolation threshold, the QN exhibits a percolation phenomenon characterized by the emergence of a giant cluster spanning the entire network. In the presence of such a giant cluster, any two arbitrary nodes in the system are connected by a chain of links with a non-zero probability, thus establishing EPR pairs at remote nodes. This work introduces a procedure for obtaining QNs from initially isolated quantum nodes. In the proposed procedure, two copies of EPR pairs are prepared at a source node and two qubits, one from each pair, are sent to a neighboring node through a noisy quantum channel. Then, a pair of mixed quantum states is established between the source node and the neighboring node. By performing local operations and classical communication, an EPR pair can be established between these two nodes with non-zero probability. Repeating this procedure for every pair of source node and neighboring node, a QN exhibiting a percolation phenomenon can be obtained.**

***Index Terms*—Quantum network, quantum noise, percolation theory, entanglement.**

I. Introduction

Quantum networks (QNs) represent a leap forward in building resources for quantum computing, communication, and sensing. A quantum network (QN) consists of nodes and links, respectively symbolizing quantum devices and pairs of quantum bits (qubits) in an arbitrary two-qubit quantum state shared between two nodes. The qubit is a basic unit of quantum information realized with a two-level quantum system [1]–[9]. In a QN, it is assumed that each pair of neighboring nodes shares a pair of qubits in a partially entangled two-qubit state, which is referred to as an entangled qubit pair (EQP). An EQP shared between any two nodes can be converted into an Einstein–Podolsky–Rosen (EPR) pair representing a pair of qubits in a maximally entangled state, known as an EPR state, by local operations and classical communication (LOCC).[1] This transformation successfully occurs with a certain probability, referred to as a singlet conversion probability (SCP) [10], [11], which can serve as a bond occupation probability in classical percolation theory [12], [13]. When an EPR state is established between two nodes, the two nodes are considered to be connected by an occupied bond and therefore are able to exchange one-qubit quantum information via LOCC. If the SCP surpasses the percolation threshold, percolation phenomena known as classical entanglement percolation (CEP) arise. Thus, a lower percolation threshold implies a higher probability of establishing long-distance entanglement between any pair of nodes. Lowering the percolation threshold in quantum systems has been a significant challenge for over a decade. The threshold of a random percolation transition is solely determined by the network topology, which is defined by the connections between nodes within the system. Consequently, altering the network topology is crucial for reducing the percolation threshold.

Research efforts, as documented in [11], [14], have demonstrated that modifying the entire network topology can reduce the percolation threshold of the CEP. The percolation, which benefits from quantum properties, is referred to as quantum entanglement percolation (QEP). These investigations have successfully introduced strategies for altering the topology of QNs to reduce percolation thresholds. However, the foundational aspect of obtaining QNs, particularly from their initial stages, remains relatively unexplored.

Obtaining QNs is a fundamental challenge for the practical deployment and scalability of QN. Thus, devising techniques to obtain a QN from scratch represents an important research goal. Here, our objective is to outline a procedure for obtaining QNs in the presence of amplitude damping noisy quantum channels. In noisy QNs obtained by the proposed procedure, a chain of bi-partite entanglement can be established, allowing for long-distance entanglement between two distant nodes via entanglement swapping [15], [16]. Additionally, establishing entanglement between two nodes has potential applications in quantum error correction [17]–[21], decoherence mitiga-

The fundamental research described in this paper was supported, in part, by the National Research Foundation of Korea under Grants NRF-2021M3H3A103657313 and NRF-2022R1A4A3033401, by the Italian MUR Next Generation EU under Grant 2022JES5S2, and by the National Science Foundation under Grant CCF-1956211. *Corresponding author: Moe Z. Win (e-mail: moewin@mit.edu).*

[1] In this study, an EPR state (or singlet state) denotes a state described by the ket $|\phi^+\rangle$, which is one of the four Bell states, since Bell states can be converted into each other by LOCC.

979-8-3503-6677-8/24/$31.00 ©2024 IEEE
DOI 10.1109/QCNC62729.2024.00031

tion [22]–[24], quantum routing [25], [26], and quantum internet [27]–[30].

This research lays the groundwork for obtaining a noisy quantum system facilitating the creation of long-distance entanglement. The key contributions of this paper are as follows:

- describing the process of obtaining QNs from initially isolated nodes in the presence of amplitude damping channels; and
- confirming that the formed QNs can exhibit entanglement percolation phenomena depending on the amount of amplitude damping quantum noise.

The remaining sections are organized as follows: Section II briefly introduces percolation theory in non-quantum networks and QNs. Section III outlines the conventional definition of entanglement percolation in noiseless QNs. Section IV provides a strategy for obtaining QNs in the presence of amplitude damping quantum noise. The corresponding entanglement percolation phenomena in the noisy QNs are described at the end of Section IV. Section V provides final remarks.

Notations: For a positive integer $n > 1$, $\mathbb{Z}_n$ denotes the set $\{0, 1, 2, \ldots, n-1\}$. Quantum states and quantum density operators are denoted by bold lowercase letters, e.g., $|\boldsymbol{\phi}\rangle$. Quantum operators and quantum density operators are both denoted by bold uppercase letter, e.g., $\boldsymbol{\Xi}$. The notation $\boldsymbol{A}^\dagger$ denotes the Hermitian adjoint of a linear operator $\boldsymbol{A}$. All these quantities are defined in connection to some finite-dimensional Hilbert space. The identity operator is denoted by $\boldsymbol{I}$ on a single-qubit Hilbert space. The symbol $\otimes$ denotes the tensor product.

II. Rudiments of Percolation Theory

A. Preliminaries on Percolation Model

A system formed by multiple interacting individual units is referred to as a complex system. Such a complex system can be effectively represented using a network model comprising nodes (also known as vertices) and links (or edges), symbolizing the individual units and their interactions, respectively. In cases where nodes are arranged regularly in a given dimensional space and links are established between adjacent nodes, the system is referred to as a lattice network. In a lattice network, a link (or bond) between two nodes is said to be occupied when interactions take place between them, which occurs with a specified bond occupation probability, and is empty otherwise. When bonds between neighboring nodes are occupied, the nodes coalesce into a cluster of connected nodes. Consequently, a giant cluster of connected nodes[2], spanning the entire system, emerges if the bond occupation probability surpasses a critical threshold known as percolation threshold. This phenomenon, known as percolation transition in percolation theory, explains the formation of a giant cluster within complex systems [12], [13]. The described percolation model has been applied to various real-world phenomena, including transitions in protein-protein interaction [31]–[37], coauthorship [38]–[42], and communication networks [43]–[46].

[2] A cluster of connected nodes, whose size is proportional to the system size, is referred to as a giant cluster.

B. Non-quantum Networks

Consider a network consisting of nodes that symbolize individual units and links that denote possible interactions among units. Links facilitate connectivity between any two nodes, determining the network's topology. A bond between two nodes is considered occupied if the two nodes interact, and empty if they do not interact. A *cluster* denotes a group of connected nodes where any two nodes within the cluster can interact via a chain of occupied bonds. Assume that each bond in the network is occupied independently with probability p, regardless of the other bonds' status. Thus, a giant cluster spanning the entire network emerges if $p \geqslant p_{\mathrm{c}}$, while the network only contain small clusters when $p < p_{\mathrm{c}}$. In such a random percolation, the critical value p_{c} is characteristic of the given network and is referred to as the percolation threshold [12], [13].

C. Quantum Networks

Consider a QN where each node functions as a quantum repeater. These repeaters are devices designed to generate EPR pairs, which are pure maximally-entangled pairs of qubits, and to execute quantum operations. A qubit of an EPR pair locally generated at one quantum node can be sent to an adjacent node through a noisy quantum channel. The amount of entanglement of the EQPs shared between neighboring nodes is determined by the noise level of quantum channel. A pair of qubits in a two-qubit quantum state shared between two adjacent nodes represents a bond, also referred to as a link or an edge within the network. A bond is considered occupied if two nodes share an EPR pair while a bond is empty if two nodes share a pair of qubits in a state different from an EPR state. When a bond between two nodes is occupied, the two nodes are merged into a cluster of connected nodes.

The EQP shared between two nodes, following the transmission of one qubit from a locally generated EPR pair through a noisy quantum channel, is described by a mixed state. Through a purification procedure [47]–[49], multiple EQPs, each described by a mixed state, can be transformed into an EQP characterized by a pure state. Likewise, multiple EQPs, each described by a pure state, can be converted into an EPR pair through a singlet conversion procedure [10], [50], [51]. Hence, by employing the combination of purification and singlet conversion procedures, it is possible to convert multiple EQP described by mixed states into an EPR pair. This combination is achieved via LOCC and succeeds with probability $p \in [0, 1]$.

If p exceeds the percolation threshold of the network, a giant cluster spanning the entire network emerges, enabling the establishment of EPR pairs between any two arbitrary nodes of the network through entanglement swapping at intermediate nodes along the chain connecting the two nodes [11]. The value of p depends on the noise level of the quantum channels.

III. Entanglement Percolation in Noiseless QNs

This section presents a preliminary scenario featuring noiseless quantum channels for connecting quantum nodes within a QN. The quantum nodes, representing quantum devices, have the capability to generate partially-entangled pair of qubits.

Consider two adjacent nodes, named Alice and Bob. Alice generates an EQP that exists in a partially-entangled pure state, described by the ket

$$|\boldsymbol{\phi}(\lambda_0)\rangle = \sqrt{\lambda_0}\,|00\rangle + \sqrt{\lambda_1}\,|11\rangle\,, \tag{1}$$

where the Schmidt coefficients λ_0 and λ_1 satisfy $\lambda_0 \geqslant \lambda_1 \geqslant 0$ and $\lambda_0 + \lambda_1 = 1$ [52]. Note that $\lambda_0 \in [1/2, 1]$ and $\lambda_1 \in [0, 1/2]$. Two Z-basis states $|0\rangle$ and $|1\rangle$ satisfy

$$\boldsymbol{X}|0\rangle = |1\rangle, \quad \boldsymbol{X}|1\rangle = |0\rangle\,, \tag{2a}$$
$$\boldsymbol{Y}|0\rangle = \imath|1\rangle, \quad \boldsymbol{Y}|1\rangle = -\imath|0\rangle\,, \tag{2b}$$
$$\boldsymbol{Z}|0\rangle = |0\rangle, \quad \boldsymbol{Z}|1\rangle = -|1\rangle\,, \tag{2c}$$

where $\imath = \sqrt{-1}$ and the quantum operators $\boldsymbol{X}$, $\boldsymbol{Y}$, and $\boldsymbol{Z}$ are known as Pauli operators [52].

Alice transmits one qubit of a locally generated EQP to Bob through an ideal quantum channel, establishing a shared EQP between them. This procedure is repeated among all pairs of neighboring nodes within the QN, ensuring each pair shares an EQP described by (1).

The partially entangled state described by (1) can be transformed into either the maximally-entangled state

$$|\boldsymbol{\phi}^+\rangle \triangleq |\boldsymbol{\phi}(1/2)\rangle = \frac{1}{\sqrt{2}}\left(|00\rangle + |11\rangle\right), \tag{3}$$

or the separable state $|00\rangle$. This transformation can be achieved by performing a measurement on a single qubit of the EQP employing the measurement operators [10], [50], [51]

$$\boldsymbol{M}_0 = \sqrt{\lambda_1/\lambda_0}\,|0\rangle\langle 0| + |1\rangle\langle 1|\,, \tag{4a}$$
$$\boldsymbol{M}_1 = \sqrt{1-\lambda_1/\lambda_0}\,|0\rangle\langle 0|\,, \tag{4b}$$

with $\boldsymbol{M}_0^\dagger \boldsymbol{M}_0 + \boldsymbol{M}_1^\dagger \boldsymbol{M}_1 = \sum_{i\in\mathbb{Z}_2} |i\rangle\langle i| = \boldsymbol{I}$. The measurement outcomes can correspond to either $\boldsymbol{M}_0$ (representing the maximally-entangled state $|\boldsymbol{\phi}^+\rangle$) or $\boldsymbol{M}_1$ (indicating the separable state $|00\rangle$), with the probabilities of occurrence being $p = 2\lambda_1$ and $1-p$, respectively. The probability p is referred to as the SCP. After performing the measurement with the operators (4a) and (4b), each bond between two neighboring nodes is occupied with probability $p = 2\lambda_1$ and empty with probability $1-p$. Note that the occupancy status of any bond is independent on the occupancy status of any other bonds within the QN. According to percolation theory, a chain of occupied bonds connecting any two distant nodes in the QN exists with a non-zero probability provided that $p > p_{\mathrm{c}}$, where p_{c} is the percolation threshold of the network [12], [13].

IV. Entanglement Percolation in Noisy QNs

This section describes a scenario involving the presence of noisy quantum channels between quantum nodes within a QN. These quantum nodes have the ability to generate an EPR pair. However, due to the noisy nature of the channels, the EQPs shared between neighboring nodes are partially-entangled qubit pairs. This section also introduces an entanglement purification protocol aimed at converting these partially entangled pairs into maximally entangled ones.

A. Sharing Two Qubits

Consider two adjacent nodes, named Alice and Bob. Alice generates an EPR pair, which is an EQP in a maximally-entangled pure state described by the ket (3). Then, Alice transmits the initial qubit of the locally generated EQP to Bob through an amplitude damping channel, which is defined by the Kraus operators

$$\boldsymbol{E}_0 = |0\rangle\langle 0| + \sqrt{1-\zeta}\,|1\rangle\langle 1|\,, \tag{5a}$$
$$\boldsymbol{E}_1 = \sqrt{\zeta}\,|0\rangle\langle 1|\,, \tag{5b}$$

with $\boldsymbol{E}_0^\dagger \boldsymbol{E}_0 + \boldsymbol{E}_1^\dagger \boldsymbol{E}_1 = \boldsymbol{I}$, where $\zeta \in [0, 1]$ is a parameter that quantifies the energy dissipation caused by the channel [47], [48], [52]. Alice and Bob finally share an EQP in the mixed state

$$\begin{aligned}\boldsymbol{\Xi}(\zeta) &= \sum_{i\in\mathbb{Z}_2} \left(\boldsymbol{E}_i \otimes \boldsymbol{I}\right) |\boldsymbol{\phi}^+\rangle\langle\boldsymbol{\phi}^+| \left(\boldsymbol{E}_i^\dagger \otimes \boldsymbol{I}\right) \\ &= \delta_0\,|\boldsymbol{\phi}(\mu_0)\rangle\langle\boldsymbol{\phi}(\mu_0)| + \delta_1\,|01\rangle\langle 01|\,,\end{aligned} \tag{6}$$

where

$$\mu_0 = 1/(2-\zeta)\,, \tag{7a}$$
$$\delta_0 = 1 - \zeta/2\,, \tag{7b}$$

$\mu_1 = 1-\mu_0$, and $\delta_1 = 1-\delta_0$ with $\mu_0 \in [1/2, 1]$ and $\delta_0 \in [1/2, 1]$.[3] The whole procedure is schematically depicted in Fig. 1(a). Note that two neighboring nodes share the EPR pair and are always connected by an occupied bond when ζ is equal to zero.

B. Generating an EPR State

The procedure outlined in Section IV-A can be repeated to obtain multiple copies of the EQP described by the density operator (6). Consider two such copies. In general, the amplitude damping quantum channel between Alice and Bob may vary over time. In such cases, the parameter ζ characterizing the channel may assume different values, denoted as $\acute{\zeta}$ and $\grave{\zeta}$, at two different time instants when the channel is utilized. Consequently, Alice and Bob share the two EQPs described by the density operators $\boldsymbol{\Xi}(\acute{\zeta})$ and $\boldsymbol{\Xi}(\grave{\zeta})$. These two mixed states are referred to as purifiable mixed states (PMSs) as they can be *purified* to obtain a single EQP with stronger entanglement than either of the two original pairs.

The initial operation of the entanglement purification protocol involves applying the CNOT operator on the two qubits in the possession of Alice and Bob. The qubits described by $\boldsymbol{\Xi}(\acute{\zeta})$ serve as control qubits, while the qubits described by $\boldsymbol{\Xi}(\grave{\zeta})$ serve as target qubits. Following this operation, the two target qubits are measured in the Z-basis. Each measurement

[3]For notational simplicity, the dependence of μ_k and δ_k with $k = 0, 1$ on ζ is not made explicit. The parameter μ_1 is defined for later use.

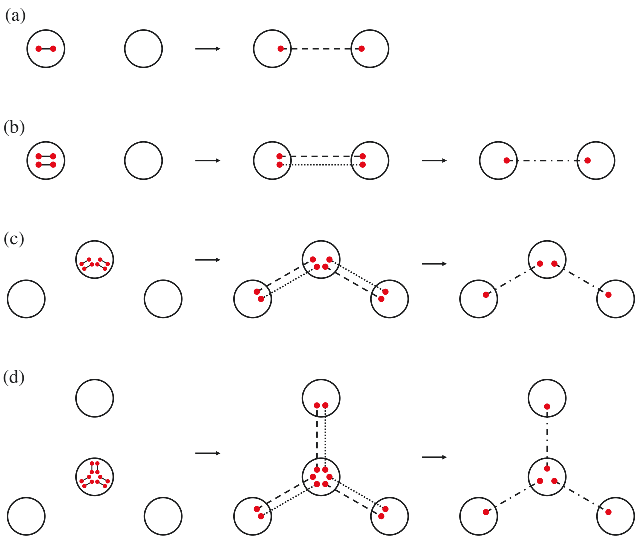

Fig. 1. (a) In a process of sharing two qubits (red circles) between two neighboring nodes (black empty circles), one qubit of an EPR pair (solid line) prepared at a source node is sent to another node through a amplitude damping noisy quantum channel. Then, the two nodes share two qubits in a mixed state (dashed line). In a process of generating an EPR state between a source node and its neighboring nodes for (b) $n = 1$, (c) $n = 2$, and (d) $n = 3$, n copies of two EPR pairs are prepared at the source node and one qubit from each pair is sent to the neighboring node through a noisy amplitude damping channel. The source node and each adjacent node can share two pairs of qubits in two different mixed states (dashed and dotted lines). Following the entanglement purification, each pair of the two mixed states undergoes transformation into one of four possible final states (dash-dotted line). Finally, the EPR state can be established from the final states with probability $P(\boldsymbol{\zeta})$.

yields two possible outcomes, corresponding to the basis elements $|0\rangle$ and $|1\rangle$, resulting in a total of four possible outcomes.

Define $\boldsymbol{\zeta} = \left(\acute{\zeta}, \grave{\zeta}\right)$. The two measurement outcomes align and correspond to $|1\rangle$ and $|1\rangle$ with probability[4]

$$Q_{\mathrm{p}}\left(\boldsymbol{\zeta}\right) = \acute{\delta}_0 \grave{\delta}_0 \left(\acute{\mu}_0 \grave{\mu}_1 + \grave{\mu}_0 \acute{\mu}_1\right), \tag{8}$$

in which case the two non-measured qubits collapse into a pure state described by the ket $|\boldsymbol{\phi}\left(\mu_{\mathrm{p},0}\right)\rangle$ where

$$\mu_{\mathrm{p},0} = 1 - \mu_{\mathrm{p},1} = \frac{\acute{\mu}_0 \grave{\mu}_1}{\acute{\mu}_0 \grave{\mu}_1 + \grave{\mu}_0 \acute{\mu}_1}. \tag{9}$$

The two measurement outcomes align and correspond to $|0\rangle$ and $|0\rangle$ with probability

$$Q_{\mathrm{m}}\left(\boldsymbol{\zeta}\right) = \acute{\delta}_0 \grave{\delta}_0 \left(\acute{\mu}_0 \grave{\mu}_0 + \acute{\mu}_1 \grave{\mu}_1\right) + \acute{\delta}_1 \grave{\delta}_1, \tag{10}$$

in which case the two non-measured qubits collapse into a new PMS

$$\boldsymbol{\Xi}_{\mathrm{m}}\left(\boldsymbol{\zeta}\right) = \delta_{\mathrm{m},0} \, |\boldsymbol{\phi}\left(\mu_{\mathrm{m},0}\right)\rangle\langle\boldsymbol{\phi}\left(\mu_{\mathrm{m},0}\right)| + \delta_{\mathrm{m},1} \, |01\rangle\langle 01| \,, \tag{11}$$

[4]The definitions of $\acute{\delta}_k$, $\acute{\mu}_k$ and $\grave{\delta}_k$, $\grave{\mu}_k$ with $k = 0, 1$, are as in (7) with ζ replaced by $\acute{\zeta}$ and $\grave{\zeta}$, respectively.

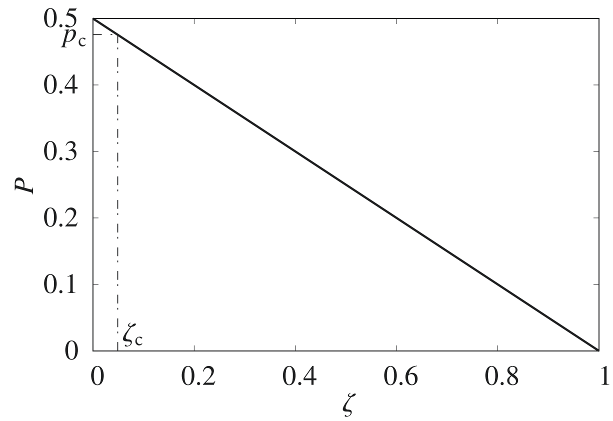

Fig. 2. Probability $P(\boldsymbol{\zeta})$ as a function of $\zeta \in (0, 1]$ (solid line) when $\zeta = \acute{\zeta} = \grave{\zeta}$. The dash-dotted guidelines indicate the percolation threshold p_{c} and the corresponding ζ_{c} in the QN for the dice lattice.

where

$$\mu_{\mathrm{m},0} = 1 - \mu_{\mathrm{m},1} = \frac{\acute{\mu}_0 \grave{\mu}_0}{\acute{\mu}_0 \grave{\mu}_0 + \acute{\mu}_1 \grave{\mu}_1}, \tag{12a}$$

$$\delta_{\mathrm{m},0} = 1 - \delta_{\mathrm{m},1} = \frac{\acute{\delta}_0 \grave{\delta}_0 \left(\acute{\mu}_0 \grave{\mu}_0 + \acute{\mu}_1 \grave{\mu}_1\right)}{Q_{\mathrm{m}}\left(\boldsymbol{\zeta}\right)}. \tag{12b}$$

In the remaining two cases, the results of the measurements do not align, which occurs with probability

$$Q_{\mathrm{r}}\left(\boldsymbol{\zeta}\right) = 1 - Q_{\mathrm{p}}\left(\boldsymbol{\zeta}\right) - Q_{\mathrm{m}}\left(\boldsymbol{\zeta}\right). \tag{13}$$

In these cases, the two non-measured qubits collapse into a mixed state that is not in the PMS form.

The outlined procedure is termed as a pure-state conversion measurement (PCM) [53]. In PCM, two distinct mixed states are purified into one pure state with probability $Q_{\mathrm{p}}\left(\boldsymbol{\zeta}\right)$ given by (8). As shown in Section III, the purified state $|\boldsymbol{\phi}\left(\mu_{\mathrm{p}}\right)\rangle$ can be converted into the EPR state $|\boldsymbol{\phi}^{+}\rangle$ described by (3) with probability $2\mu_{\mathrm{p},1}$. Consequently, the total probability $P(\boldsymbol{\zeta})$ of obtaining the EPR state from two mixed states $\boldsymbol{\Xi}\left(\acute{\zeta}\right)$ and $\boldsymbol{\Xi}\left(\grave{\zeta}\right)$ is given by

$$P(\boldsymbol{\zeta}) = \begin{cases} 1, & \text{for } \acute{\zeta} = 0 \text{ or } \grave{\zeta} = 0\,, \\ 2\grave{\mu}_0 \acute{\mu}_1 \acute{\delta}_0 \grave{\delta}_0\,, & \text{for } \acute{\zeta}, \grave{\zeta} \in (0, 1]\,. \end{cases} \tag{14}$$

Note that $P(\boldsymbol{\zeta})$ can be rewritten as $P(\boldsymbol{\zeta}) = (1 - \zeta)/2$ for $\zeta = \acute{\zeta} = \grave{\zeta} \in (0, 1]$, as shown in Fig. 2.

Additionally, consider that n copies of two EPR pairs are generated at a specific source node and each copy is then shared with one of the n neighboring nodes. To achieve this sharing, one qubit from each EPR pair is transmitted to the neighboring node through a noisy quantum channel, resulting in the formation of two mixed states between the source node and each neighboring node. After performing entanglement purification on these mixed states, the source node and each neighboring node share an EPR pair with probability $P(\boldsymbol{\zeta})$. Fig. 1 (b), (c), and (d) depict the method for generating an EPR state for $n = 1$, $n = 2$, and $n = 3$, respectively.

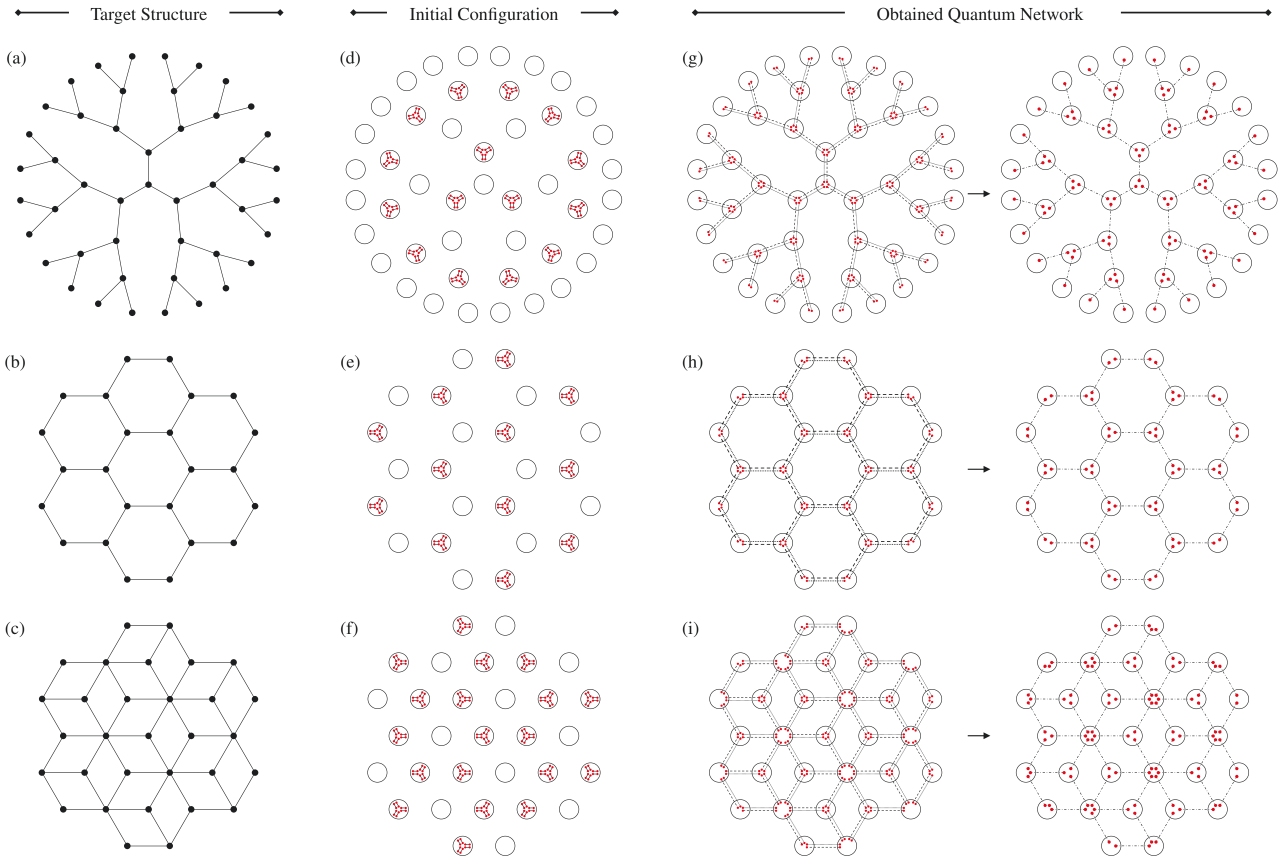

Fig. 3. The lattice structures considered in this work are (a) Bethe, (h) honeycomb, and (i) dice lattices, with nodes and bonds are represented by filled circles and solid lines, respectively. Three copies of two EPR pairs, each pair of which is in an EPR state (solid line), are prepared at each of all source nodes for obtaining QNs with lattice structures of (d) Bethe, (e) honeycomb, and (f) dice lattices. After the qubit sharing process over the noisy quantum channels, two pairs of qubits in distinct mixed states (dashed and dotted lines) are shared between each pair of two adjacent nodes, forming a quantum (g) Bethe with a coordination number 3, (h) honeycomb lattice, and (i) dice lattice. Subsequently, by performing the entanglement purification protocols, each pair of two mixed states is transformed into one of 4 possible final states (dash-dotted line). Finally, each pair of two neighboring nodes can share an EPR pair with probability $P(\boldsymbol{\zeta})$.

C. *Establishing Global Entanglement in Noisy QNs*

We now consider three specific QNs with lattice structures, namely Bethe (coordination number[5] $k=3$), honeycomb, and dice lattices as shown in Fig. 3 (a), (b), and (c), respectively. Initially, each source node, positioned in correspondence to the nodes of Bethe ($k=3$), honeycomb, and dice lattices, prepares three sets of two EPR pairs, as depicted in Figs. 3 (d), (e), and (f). Then, as illustrated in Figs. 3 (g), (h), and (i), the process of sharing qubit pairs between each source node and its neighboring nodes results in the formation of a QN. In this network, every pair of adjacent nodes shares two pairs of qubits in the state $\boldsymbol{\varXi}(\acute{\zeta}) \otimes \boldsymbol{\varXi}(\grave{\zeta})$ achieved by transmitting single qubits through a time-varying amplitude damping noisy quantum channel, as outlined in Section IV-B. Finally, by employing entanglement purification protocols, each four-qubit state $\boldsymbol{\varXi}(\acute{\zeta}) \otimes \boldsymbol{\varXi}(\grave{\zeta})$ can be converted into a two-qubit EPR state $|\phi^+\rangle\langle\phi^+|$ with probability $P(\boldsymbol{\zeta})$. The probability $P(\boldsymbol{\zeta})$ corresponds to the bond occupation probability between two neighboring nodes in the QN. A giant cluster, whose size scales with the system size N, emerges when the probability $P(\boldsymbol{\zeta})$ surpasses the percolation threshold $p_{\rm c}$ of the formed network [11]–[13]. The presence of a giant cluster signifies the occurrence of percolation phenomena. Therefore, percolation phenomena occur when $P(\boldsymbol{\zeta}) \geqslant p_{\rm c}$. Assuming $\zeta = \acute{\zeta} = \grave{\zeta}$, there exists a threshold $\zeta_{\rm c}$ for the energy dissipation parameter of the channel at which the percolation phenomena begin to occur. The threshold $\zeta_{\rm c}$ is defined as the value of ζ at which $P(\boldsymbol{\zeta}) = p_{\rm c}$ if $p_{\rm c} < 1/2$, whereas $\zeta_{\rm c} = 0$ if $p_{\rm c} \geqslant 1/2$.

The percolation threshold for the Bethe lattice in which all nodes have the same coordination number k is known to be $p_{\rm c} = 1/(k-1)$ [54], [55]. Consequently, for $k=3$, the percolation threshold in the Bethe lattice equals $1/2$. The percolation thresholds in the honeycomb and dice lattices are known to be 0.6527 and 0.4756, respectively [12], [13]. The

[5]The coordination number indicates the number of nearest neighbors of a node within a specific complex system.

TABLE I
PERCOLATION THRESHOLDS p_c AND THE CORRESPONDING AMPLITUDE DAMPING THRESHOLDS ζ_c IN NOISY BETHE, HONEYCOMB, AND DICE QNS WHEN $\zeta = \acute{\zeta} = \grave{\zeta}$.

Lattice	p_c	ζ_c
Bethe ($k = 3$)	0.5	0
Honeycomb	0.6527(1)	0
Dice	0.4756(1)	0.0488(1)

corresponding values of ζ_c are 0, 0, and $0.0488(1)$ for the Bethe ($k = 3$), honeycomb, and dice quantum lattice networks, respectively. Thus, percolation phenomena are observed in the noiseless Bethe ($k = 3$) and noiseless honeycomb QNs, and in the noisy dice QN with $\zeta \leqslant 0.0488(1)$. The values of p_c with their corresponding ζ_c for the considered quantum lattice networks are presented in Table I. By utilizing the explicit expression for $P(\boldsymbol{\zeta}) = (1-\zeta)/2$ with $\zeta = \acute{\zeta} = \grave{\zeta} \in (0, 1]$, a plot of the order parameter G, which denotes the normalized largest cluster size, as a function of $\zeta \in (0, 1]$ in the noisy dice QN is shown in Fig. 4.

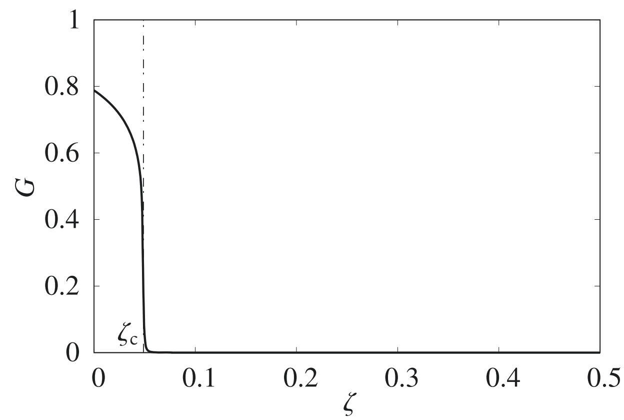

Fig. 4. Order parameter G, representing the normalized largest cluster size, as a function of $\zeta \in (0, 1]$ for (a) the noisy dice QN (solid line) when $\zeta = \acute{\zeta} = \grave{\zeta}$. The vertical dash-dotted guidelines indicate the amplitude damping thresholds ζ_c in the noisy dice QN.

V. CONCLUSION

This study has developed practical procedures to obtain QNs in the presence of amplitude damping quantum noise. The QN comprises source nodes initially generating a specific quantity of EPR pairs. These pairs are then shared with neighboring quantum nodes over noisy quantum channels. By combining entanglement purification and singlet conversion protocols, the systems may exhibit percolation phenomena depending on the level of noise in the quantum channels. When percolation phenomena occur, any pair of nodes in the system can establish long-distance entanglement with a non-zero probability via entanglement swapping. This study aids in the practical implementation of quantum systems. Our findings are anticipated to have an impact on future investigations in quantum information and quantum percolation phenomena.

REFERENCES

[1] D. L. Moehring, P. Maunz, S. Olmschenk, K. C. Younge, D. N. Matsukevich, L.-M. Duan, and C. Monroe, "Entanglement of single-atom quantum bits at a distance," *Nature*, vol. 449, no. 7158, pp. 68–71, Sep. 2007.

[2] A. Delteil, Z. Sun, W.-b. Gao, E. Togan, S. Faelt, and A. Imamoğlu, "Generation of heralded entanglement between distant hole spins," *Nature Physics*, vol. 12, no. 3, pp. 218–223, Mar. 2016.

[3] R. Stockill, M. Stanley, L. Huthmacher, E. Clarke, M. Hugues, A. Miller, C. Matthiesen, C. Le Gall, and M. Atatüre, "Phase-Tuned Entangled State Generation between Distant Spin Qubits," *Physical Review Letters*, vol. 119, no. 1, p. 010503, Jul. 2017.

[4] J. Hofmann, M. Krug, N. Ortegel, L. Gérard, M. Weber, W. Rosenfeld, and H. Weinfurter, "Heralded Entanglement Between Widely Separated Atoms," *Science*, vol. 337, no. 6090, pp. 72–75, Jul. 2012.

[5] S. Ritter, C. Nölleke, C. Hahn, A. Reiserer, A. Neuzner, M. Uphoff, M. Mücke, E. Figueroa, J. Bochmann, and G. Rempe, "An elementary quantum network of single atoms in optical cavities," *Nature*, vol. 484, no. 7393, pp. 195–200, Apr. 2012.

[6] H. Bernien, B. Hensen, W. Pfaff, G. Koolstra, M. S. Blok, L. Robledo, T. H. Taminiau, M. Markham, D. J. Twitchen, L. Childress, and R. Hanson, "Heralded entanglement between solid-state qubits separated by three metres," *Nature*, vol. 497, no. 7447, pp. 86–90, May 2013.

[7] P. C. Humphreys, N. Kalb, J. P. J. Morits, R. N. Schouten, R. F. L. Vermeulen, D. J. Twitchen, M. Markham, and R. Hanson, "Deterministic delivery of remote entanglement on a quantum network," *Nature*, vol. 558, no. 7709, p. 268, 2018.

[8] S. Guerrini, M. Z. Win, M. Chiani, and A. Conti, "Quantum Discrimination of Noisy Photon-Added Coherent States," *IEEE Journal on Selected Areas in Information Theory*, vol. 1, no. 2, pp. 469–479, Aug. 2020.

[9] S. Guerrini, M. Z. Win, and A. Conti, "Photon-varied quantum states: Unified characterization," *Physical Review A*, vol. 108, no. 2, p. 022425, Aug. 2023.

[10] G. Vidal, "Entanglement of pure states for a single copy," *Phys. Rev. Lett.*, vol. 83, no. 5, pp. 1046–1049, Aug. 1999.

[11] A. Acín, J. I. Cirac, and M. Lewenstein, "Entanglement percolation in quantum networks," *Nat. Physics*, vol. 3, no. 4, pp. 256–259, Feb. 2007.

[12] D. Stauffer and A. Aharony, *Introduction to percolation theory*. Taylor & Francis, 1994.

[13] K. Christensen and N. R. Moloney, *Complexity and Criticality*. World Scientific Publishing Company, 2005.

[14] S. Perseguers, D. Cavalcanti, G. J. Lapeyre, M. Lewenstein, and A. Acín, "Multipartite entanglement percolation," *Physical Review A*, vol. 81, no. 3, p. 032327, Mar. 2010.

[15] Z. Liu, S. Marano, and M. Z. Win, "An Asymptotically Achievable Rate Bound for Establishing High-Fidelity Entanglements in Quantum Networks," in *ICASSP 2024 - 2024 IEEE International Conference on Acoustics, Speech and Signal Processing (ICASSP)*, Apr. 2024, pp. 9271–9275.

[16] ——, "Establishing High-Fidelity Entanglement in Quantum Repeater Chains," *IEEE Journal on Selected Areas in Communications*, pp. 1–1, 2024.

[17] P. W. Shor, "Scheme for reducing decoherence in quantum computer memory," *Phys. Rev. A*, vol. 52, no. 4, pp. R2493–R2496, Oct. 1995.

[18] A. S. Fletcher, P. W. Shor, and M. Z. Win, "Structured near-optimal channel-adapted quantum error correction," *Physical Review A*, vol. 77, no. 1, p. 012320, Jan. 2008.

[19] T. Brun, I. Devetak, and M.-H. Hsieh, "Correcting Quantum Errors with Entanglement," *Science*, vol. 314, no. 5798, pp. 436–439, Oct. 2006.

[20] A. S. Fletcher, P. W. Shor, and M. Z. Win, "Channel-Adapted Quantum Error Correction for the Amplitude Damping Channel," *IEEE Transactions on Information Theory*, vol. 54, no. 12, pp. 5705–5718, Feb. 2008.

[21] M. Chiani, A. Conti, and M. Z. Win, "Piggybacking on quantum streams," *Physical Review A*, vol. 102, no. 1, p. 012410, Jul. 2020.

[22] P. Mandayam, K. Jagannathan, and A. Chatterjee, "The classical capacity of additive quantum queue-channels," *IEEE J. Sel. Areas Inf. Theory*, vol. 1, no. 2, pp. 432–444, Aug. 2020.

[23] S. Brand, T. Coopmans, and D. Elkouss, "Efficient computation of the

waiting time and fidelity in quantum repeater chains," *IEEE J. Sel. Areas Commun.*, vol. 38, no. 3, pp. 619–639, Mar. 2020.

[24] S. Marano and M. Z. Win, "Distributing quantum states with finite lifetime," *Physical Review A*, vol. 107, no. 5, p. 052413, May 2023.

[25] M. Pant, H. Krovi, D. Towsley, L. Tassiulas, L. Jiang, P. Basu, D. Englund, and S. Guha, "Routing entanglement in the quantum Internet," *npj Quantum Inf.*, vol. 5, no. 1, pp. 1–9, Mar. 2019.

[26] W. Shi and R. Malaney, "Quantum Routing for Emerging Quantum Networks," *IEEE Network*, pp. 1–1, 2023.

[27] N. Hosseinidehaj, Z. Babar, R. Malaney, S. X. Ng, and L. Hanzo, "Satellite-based continuous-variable quantum communications: State-of-the-art and a predictive outlook," *IEEE Commun. Surveys Tuts.*, vol. 21, no. 1, pp. 881–919, 2019.

[28] A. S. Cacciapuoti, M. Caleffi, R. Van Meter, and L. Hanzo, "When Entanglement Meets Classical Communications: Quantum Teleportation for the Quantum Internet," *IEEE Transactions on Communications*, vol. 68, no. 6, pp. 3808–3833, Jun. 2020.

[29] A. S. Cacciapuoti, M. Caleffi, F. Tafuri, F. S. Cataliotti, S. Gherardini, and G. Bianchi, "Quantum Internet: Networking Challenges in Distributed Quantum Computing," *IEEE Network*, vol. 34, no. 1, pp. 137–143, Jan. 2020.

[30] M. Viscardi, J. Illiano, A. S. Cacciapuoti, and M. Caleffi, "Entanglement Distribution in the Quantum Internet: An Optimal Decision Problem Formulation," in *2023 IEEE International Conference on Quantum Computing and Engineering (QCE)*, vol. 01, Sep. 2023, pp. 1114–1119.

[31] K. I. Goh, B. Kahng, and D. Kim, "Graph theoretic analysis of protein interaction networks of eukaryotes," *Physica A: Statistical Mechanics and its Applications*, vol. 357, no. 3, pp. 501–512, 2005.

[32] I. Ispolatov, P. L. Krapivsky, and A. Yuryev, "Duplication-divergence model of protein interaction network," *Physical Review E*, vol. 71, no. 6, p. 061911, 2005.

[33] K. Evlampiev and H. Isambert, "Conservation and topology of protein interaction networks under duplication-divergence evolution," *Proceedings of the National Academy of Sciences*, vol. 105, no. 29, pp. 9863–9868, 2008.

[34] J. Kim, P. L. Krapivsky, B. Kahng, and S. Redner, "Infinite-order percolation and giant fluctuations in a protein interaction network," *Physical Review E*, vol. 66, p. 055101, Nov. 2002.

[35] S. M. Oh, S.-W. Son, and B. Kahng, "Suppression effect on the Berezinskii-Kosterlitz-Thouless transition in growing networks," *Physical Review E*, vol. 98, no. 6, p. 060301, Dec. 2018.

[36] S. Dahiya, V. Saini, P. Kumar, and A. Kumar, "Protein-Protein interaction network analyses of human WNT proteins involved in neural development," *Bioinformation*, vol. 15, no. 5, pp. 307–314, Apr. 2019.

[37] S. M. Oh, S.-W. Son, and B. Kahng, "Discontinuous percolation transitions in growing networks," *Journal of Statistical Mechanics: Theory and Experiment*, vol. 2019, no. 8, p. 083502, Aug. 2019.

[38] M. E. J. Newman, "The structure of scientific collaboration networks," *Proceedings of the National Academy of Sciences*, vol. 98, no. 2, pp. 404–409, Jan. 2001.

[39] J. Moody, "The structure of a social science collaboration nnetwork: Disciplinary cohesion from 1963 to 1999," *American Sociological Review*, vol. 69, no. 2, pp. 213–238, Apr. 2004.

[40] M. E. J. Newman, "Coauthorship networks and patterns of scientific collaboration," *Proceedings of the National Academy of Sciences*, vol. 101, no. suppl 1, pp. 5200–5205, Apr. 2004.

[41] D. Lee, K.-I. Goh, B. Kahng, and D. Kim, "Complete trails of coauthorship network evolution," *Physical Review E*, vol. 82, p. 026112, Aug. 2010.

[42] S. Fortunato, C. T. Bergstrom, K. Börner, J. A. Evans, D. Helbing, S. Milojević, A. M. Petersen, F. Radicchi, R. Sinatra, B. Uzzi, A. Vespignani, L. Waltman, D. Wang, and A.-L. Barabási, "Science of science," *Science*, vol. 359, no. 6379, Mar. 2018.

[43] E. N. Gilbert, "Random plane networks," *Journal of the Society for Industrial and Applied Mathematics*, vol. 9, p. 533, 1961.

[44] M. D. Penrose, "On a continuum percolation model," *Advances in Applied Probability*, vol. 23, no. 3, pp. 536–556, 1991.

[45] O. Dousse, M. Franceschetti, N. Macris, R. Meester, and P. Thiran, "Percolation in the signal to interference ratio graph," *Journal of Applied Probability*, vol. 43, no. 2, pp. 552–562, 2006.

[46] P. C. Pinto and M. Z. Win, "Percolation and Connectivity in the Intrinsically Secure Communications Graph," *IEEE Transactions on Information Theory*, vol. 58, no. 3, pp. 1716–1730, Mar. 2012.

[47] S. Broadfoot, U. Dorner, and D. Jaksch, "Entanglement percolation with bipartite mixed states," *Europhysics Letters*, vol. 88, no. 5, p. 50002, Dec. 2009.

[48] L. Ruan, W. Dai, and M. Z. Win, "Adaptive recurrence quantum entanglement distillation for two-Kraus-operator channels," *Physical Review A*, vol. 97, no. 5, p. 052332, May 2018.

[49] L. Ruan, B. T. Kirby, M. Brodsky, and M. Z. Win, "Efficient entanglement distillation for quantum channels with polarization mode dispersion," *Physical Review A*, vol. 103, no. 3, Mar. 2021.

[50] M. A. Nielsen, "Conditions for a class of entanglement transformations," *Phys. Rev. Lett.*, vol. 83, no. 2, pp. 436–439, Jul. 1999.

[51] M. Siomau, "Quantum entanglement percolation," *Journal of Physics B: Atomic, Molecular and Optical Physics*, vol. 49, no. 17, p. 175506, 2016.

[52] M. A. Nielsen and I. L. Chuang, *Quantum Computation and Quantum Information*. Cambridge University Press, 2000.

[53] S. Perseguers, J. I. Cirac, A. Acín, M. Lewenstein, and J. Wehr, "Entanglement distribution in pure-state quantum networks," *Physical Review A*, vol. 77, no. 2, p. 022308, Feb. 2008.

[54] R. Albert and A.-L. Barabási, "Statistical mechanics of complex networks," *Reviews of Modern Physics*, vol. 74, no. 1, pp. 47–97, Jan. 2002.

[55] T. Nogawa and T. Hasegawa, "Monte Carlo simulation study of the two-stage percolation transition in enhanced binary trees," *Journal of Physics A: Mathematical and Theoretical*, vol. 42, no. 14, p. 145001, Mar. 2009.